Steel and Composite Structures, *Vol. 33, No. 1 (2019) 19-36*
DOI: https://doi.org/10.12989/scs.2019.33.1.019

Seismic performance of composite plate shear walls with variable column flexural stiffness

Ivan Curkovic*[1], Davor Skejic[1a], Ivica Dzeba[1b] and Gianfranco De Matteis[2a]

[1] *Department of Structures, University of Zagreb, Faculty of Civil Engineering, Kaciceva 26, 10000 Zagreb, Republic of Croatia*
[2] *Department of Architecture and Industrial Design, University of Campania Luigi Vanvitelli, Abbey of San Lorenzo in Septimum, 81031 Aversa (CE), Italy*

(*Received November 14, 2018, Revised March 8, 2019, Accepted March 22, 2019*)

Abstract. Cyclic behaviour of composite (steel – concrete) plate shear walls (CPSW) with variable column flexural stiffness is experimentally and numerically investigated. The investigation included design, fabrication and testing of three pairs of one-bay one-storey CPSW specimens. The reference specimen pair was designed in way that its column flexural stiffness corresponds to the value required by the design codes, while within the other two specimen pairs column flexural stiffness was reduced by 18% and 36%, respectively. Specimens were subjected to quasi-static cyclic tests. Obtained results indicate that column flexural stiffness reduction in CPSW does not have negative impact on the overall behaviour allowing for satisfactory performance for up to 4% storey drift ratio while also enabling inelastic buckling of the infill steel plate. Additionally, in comparison to similar steel plate shear wall (SPSW) specimens, column "pull-in" deformations are less pronounced within CPSW specimens. Therefore, the results indicate that prescribed minimal column flexural stiffness value used for CPSW might be conservative, and can additionally be reduced when compared to the prescribed value for SPSWs. Furthermore, finite element (FE) pushover simulations were conducted using shell and solid elements. Such FE models can adequately simulate cyclic behaviour of CPSW and as such could be further used for numerical parametric analyses. It is necessary to mention that the implemented pushover FE models were not able to adequately reproduce column "pull-in" deformation and that further development of FE simulations is required where cyclic loading of the shear walls needs to be simulated.

Keywords: composite plate shear wall; infill panel shear yield; quasi-static cyclic test; column flexural stiffness; finite element model

1. Introduction

In past several decades, numerous experimental and numerical investigations on steel plate shear walls (SPSWs) have been conducted. Those research demonstrated that, due to its ductility, SPSWs are particularly suitable to be used as building lateral load resisting systems (Thorburn *et al*. 1983, Elgaaly *et al*. 1993, Driver *et al*. 1998, Lubell *et al*. 2000, Sabelli and Bruneau 2007). However, SPSWs typically consist of thin infill steel plate connected to columns (vertical boundary elements (VBEs)), and beams (horizontal boundary elements (HBEs)) and when loaded they tend to buckle in shear at very early stage (Wagner 1931). Buckling of the plate in shear before it has yielded reduces the system overall strength, stiffness and energy dissipation capacity. Therefore, the idea has sprung to preclude infill plate buckling by increasing steel plate thickness, using various types of infills (e.g., corrugated webs (Kalali *et al*. 2014)) or by using numerous stiffeners (common in Japan) (e.g., Rahmzadeh *et al*. 2016). In addition, in order to anticipate shear plastic deformation of the plate the use of low-yield strength steel and pure aluminium (De Matteis *et al*. 2003, 2007, 2008), as well as the use of perforated plates (De Matteis *et al*. 2016,), has been proposed. However, all of these approaches imply significant increase in costs.

In order to effectively prevent early infill plate buckling, as an alternative to all metal solutions presented by Brando *et al*. (2013), Astaneh-Asl (2002), proposed use of reinforced concrete (RC) panel which would be connected to the infill steel plate at discrete points. As the steel infill plate and RC panel work together to transfer the loads the system was termed composite plate shear wall (CPSW) system. Additionally, Astaneh-Asl also proposed innovative type of CPSW system where the RC panel would not be engaged with the surrounding boundary elements, as it was the case with the traditional systems, but rather that a small gap between RC panel and the frame exists. In that way, the RC panel is completely taken out of the load bearing mechanism, and its sole purpose is to restrain the infill plate in the out-of-plane direction.

Both, SPSWs and CPSWs, design procedures are based on capacity design approach where all structural elements are designed using resistance (capacity) of one predefined structural member. The relevant member governing the design is, in the vast majority cases, the one carrying most of the load and/or the one where the most of the inelasticity,

*Corresponding author, Ph.D.,
E-mail: icurkovic@grad.hr
[a] Associate Professor
[b] Professor

ISSN: 1229-9367 (Print), 1598-6233 (Online)

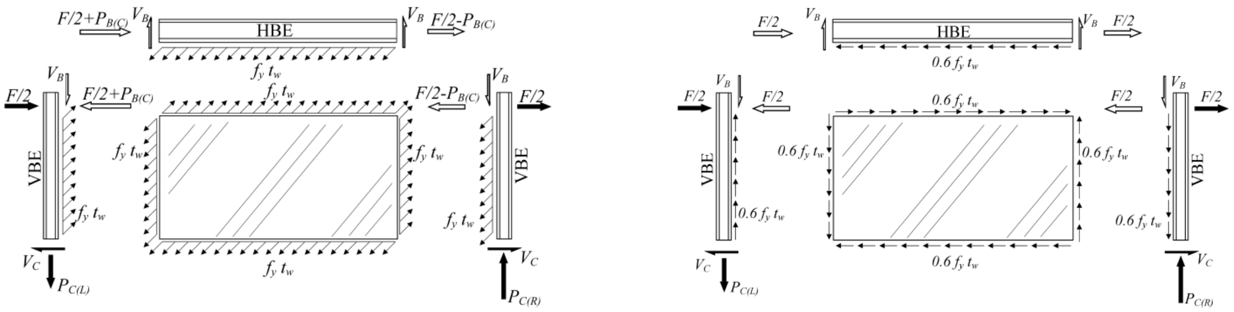

(a) Steel plate shear wall

(b) Composite plate shear wall

Fig. 1 Stress distribution from infill to boundary elements (Sabelli and Bruenau 2007, Curkovic 2017)

i.e., energy dissipation, occurs. The relevant members of SPSWs and CPSWs are either steel or composite infill panels, respectively. Application of the capacity design philosophy results with stress distribution as is presented in Fig. 1, where F is the applied lateral load, $P_{B(C)}$ is the axial force applied at the end of the beam due to actions on the column, $P_{C(L/R)}$ is the axial force reaction in left or right column, and V_B and V_C are the shear reactions of the beam and column due to transverse action, respectively. It is, therefore, obvious that SPSWs and CPSWs have different load bearing mechanisms. When correctly designed, SPSWs assume development of the tension field within the entire steel infill plate. However, if due to application of the RC panel steel infill panel buckling is precluded, the plate should be able to yield in shear, allowing development of greater system strength in CPSWs than in SPSWs. Omitting the load bearing capacity of the boundary frame, as is prescribed within the design standards (AISC 2010, CEN 2004), and comparing only nominal strengths of the stiffened and unstiffened steel infill plate, the strength V_n of the SPSWs is only about 70% of the CPSWs strength, which is according to AISC (2010) and CEN (2004) calculated as

$$V_n = \frac{f_y}{\sqrt{3}} L_{cf}\ t_w \approx 0{,}6\ f_y\ L_{cf}\ t_w \tag{1}$$

where t_w is the infill panel thickness, L_{cf} is the clear distance between column flanges, and f_y is the yield strength of the infill panel material. This sets CPSWs apart as systems particularly suitable for application in structures where lateral actions are significant, i.e., in the areas of high seismicity or zones with increased wind actions. Additionally, in comparison to SPSWs, due to better utilization of the steel infill plate, CPSWs provide greater energy dissipation capacity, maintaining at the same time good system ductility (Zhao and Astaneh-Asl 2004, 2007, Arabzadeh *et al*. 2011). Also, in the aftermath of moderate and more frequent earthquakes, buckling of the steel infill plate or cracking of the concrete is precluded (especially if the innovative type of CPSW is used), which is desirable as the structure can continue with its full functionality without the need for repairs, which could be incompatible with its usage and cause additional material losses (Astaneh-Asl 2002).

Currently available numerical and experimental investigations on the CPSWs have mostly been focused on the variation of composite panel characteristics and its influence on the overall behaviour of the system (Curkovic and Dzeba 2016). Within those investigations the influence of either steel plate or RC panel thickness (Arabzadeh *et al*. 2011, Shafaei *et al*. 2016, Zhao 2006, Machaly *et al*. 2014, Rahnavard *et al*. 2016, Guo *et al*. 2017), steel and concrete material characteristics (Arabzadeh *et al*. 2011, Rassouli *et al*. 2016, Zhao 2006, Machaly *et al*. 2014), connection between the steel and RC plate (Arabzadeh *et al*. 2011, Rahnavard *et al*. 2016, Qi *et al*. 2017), number of applied RC panels (Arabzadeh *et al*. 2011, Rassouli *et al*. 2016, Rahnavard *et al*. 2016), existence of the gap between RC panel and BE (Astaneh-Asl 2002, Zhao and Astaneh-Asl 2007, Arabzadeh *et al*. 2011), reinforcement ratio (Arabzadeh *et al*. 2011, Shafaei *et al*. 2016, Lie *et al*. 2018), composite panel aspect ratio, i.e., height to length ratio (Arabzadeh *et al*. 2011, Machaly *et al*. 2014, Guo *et al*. 2017), steel plate cut-outs (Jin *et al*. 2016, Shafaei *et al*. 2017), connection of the steel plate to BE (Guo *et al*. 2017, Lie *et al*. 2018, Hou *et al*. 2013, Liu *et al*. 2017, Wei *et al*. 2017), were investigated. On the other hand influence of the boundary elements and their joints on the overall CPSW system behaviour has only to an extent been investigated by few research groups, i.e., Zhao (2006), Arabzadeh *et al*. (2011), Wei *et al*. (2017), Hadzhiyaneva and Belev (2014) and Guo *et al*. (2017). In particular, Hadiyaneva and Belev (2014) studied the behaviour of CPSWs using frames with partial strength beam-to-column joints. Guo *et al*. (2017) tested CPSWs where the infill plate is connected only to HBEs. Although in their research Zhao (2006) and Arabzadeh *et al*. (2011) did not explicitly vary BE moment of inertia value, they investigated the influence of BE flexural stiffness influence on the overall system behaviour through the variation of the infill steel plate thickness. The only issue was that BE were oversized and therefore no valuable conclusions could have been derived. Recently, Wei *et al*. (2017) derived analytical expression for determination of minimum CPSWs VBE flexural stiffness allowed that is based on the expression derived for SPWSs (see Eq. (2)). The derived expression predicts reduction of the prescribed column flexural stiffness requirement for CPSWs. The expression was also validated through extensive numerical pushover analysis. Possible issue here is that the authors consider the prescribed flexural stiffness requirement of SPSW columns as legitimate condition and base their research on it. Namely, Qu and Bruneau (2010) have already analytically considered the issue regarding column flexural stiffness requirement in SPSWs. Their results showed no correlation between column flexural stiffness and significant “pull-in” deformations of VBEs. However, it is necessary that VBEs are adequately designed using only strength-based design approach, omitting therefore column flexural stiffness requirement. Even though the results showed that the current column flexural stiffness requirement might be completely excessive, they noticed that further experimental and analytical research should be conducted to confirm these findings. This was additionally confirmed by the research of Li *et al*. (2014), who again confirmed that VBEs of SPSW need to be designed using only capacity design approach, i.e., strength-based approach. On the other hand, Machaly *et al*. (2014) conducted extensive numerical parametric analyses of SPSWs under cyclic loading concluding that the current minimum column moment of inertia requirement might not be sufficient to ensure yielding of the entire infill steel plate. For that reason they recommended that the column flexural stiffness should be based on limiting column inward deflections.

Therefore, this research was conducted in order to further investigate the column flexural stiffness requirement of CPSWs. The research was divided into experimental and numerical part. Experimental investigation included testing of specimens with variable column flexural stiffness. Afterwards, the obtained experimental results served for calibration of numerical pushover models. Calibration of FE models is also necessary in order to conduct numerical parametric analysis to further investigate influence of column flexural stiffness on CPSW behaviour. The scope of this research were also moment resisting frames (MRFs) and SPSWs with variable column moment of inertia but only their key results are presented here, while more detailed results can be found in accompanying paper (Curkovic *et al*. 2019).

2. Column flexural stiffness requirement

As previously shown, CPSWs present relatively new vertical stabilization systems and therefore have not been extensively investigated. Accordingly, in the absence of a more detailed insight into their behaviour prescribed design recommendations are overtaken from the similar SPSW systems. This is also the case with the minimum column flexural stiffness requirement in AISC (2010) and CEN (2004), which has been derived from the need to provide adequate boundary supports to enable tension field development over the entire steel infill plate (Wagner 1931, Curkovic *et al*. 2019, Kuhn *et al*. 1952, Montgomery and Medhekar 2001), and is calculated as

$$I_c \geq \frac{0.0031\, t_w H^4}{L} \tag{2}$$

where H presents the storey height, t_w is the infill panel thickness and L is the SPSW or CPSW width.

Comparing stress states within the SPSW and CPSW, shown in Figs. 1(a)-(b), it is clear that CPSW has more favourable stress distribution from the infill panel to the boundary elements. Due to that unfavourable stress distribution present in SPSWs some of the authors have been investigating behavior of SPSW having various shapes and sizes of openings within the infill panel (Ali *et al*. 2018, Massumi *et al*. 2018). In CPSW case transverse stresses acting on VBEs, due to predicted load bearing mechanism, could be significantly reduced or might not even exist at all. Therefore, it has been suspected that the column moment of the inertia requirement for CPSW can be either reduced or maybe even completely omitted.

Hence, in order to evaluate suitability of code compliant column flexibility factor, i.e., application of column flexural stiffness requirement experimental and numerical investigations were conducted.

3. Experimental programme

3.1 General

The experimental research was conducted within the framework of the Ph.D. thesis (Curkovic 2017) at the Faculty of Civil Engineering at the University of Zagreb, Croatia. For that purpose three pairs of CPSW specimens with variable column flexural stiffness were tested. Additionally, within this research two other specimen groups including MRF and SPSW specimens were tested and those results can be found in Curkovic (2017) and Curkovic *et al*. (2019). SPSW specimens have been tested in order to compare their behaviour with CPSW specimens, while the testing of MRF specimens was conducted in order to determine the contribution of the steel frame alone to the stiffness and load bearing capacity of the SPSWs and CPSWs.

3.2 Preparation of the specimens

For the purpose of experimental investigations, six one-story one-bay specimens with 1:4 scale were designed and fabricated. All steel parts of the specimens were fabricated and welded at the factory after which the specimens were transported to the concrete plant where the concrete panels were poured and the concrete was cured. Afterwards, specimens were transported to the laboratory where final preparations before the testing were carried out. Width-to-height aspect ratio was approximately one, with height of the scaled specimens of 1030 mm and the bay span of 1000 mm, Fig. 2. Three CPSW specimen pairs with modified column geometry were tested.

Although CPSWs have different load bearing mechanism than SPSWs, their design is mostly, due to lack of the research, based on the design guidelines for SPSWs (Curkovic and Dzeba 2016). Therefore, design of steel parts was conducted in accordance with European norm EN 1993-1-1 (CEN 2005) while taking into account any of the requirements given for seismic design of buildings provided in EN 1998-1 (CEN 2004). Since CEN (2004) does not provide any guideline for SPSWs, design of SPSWs was

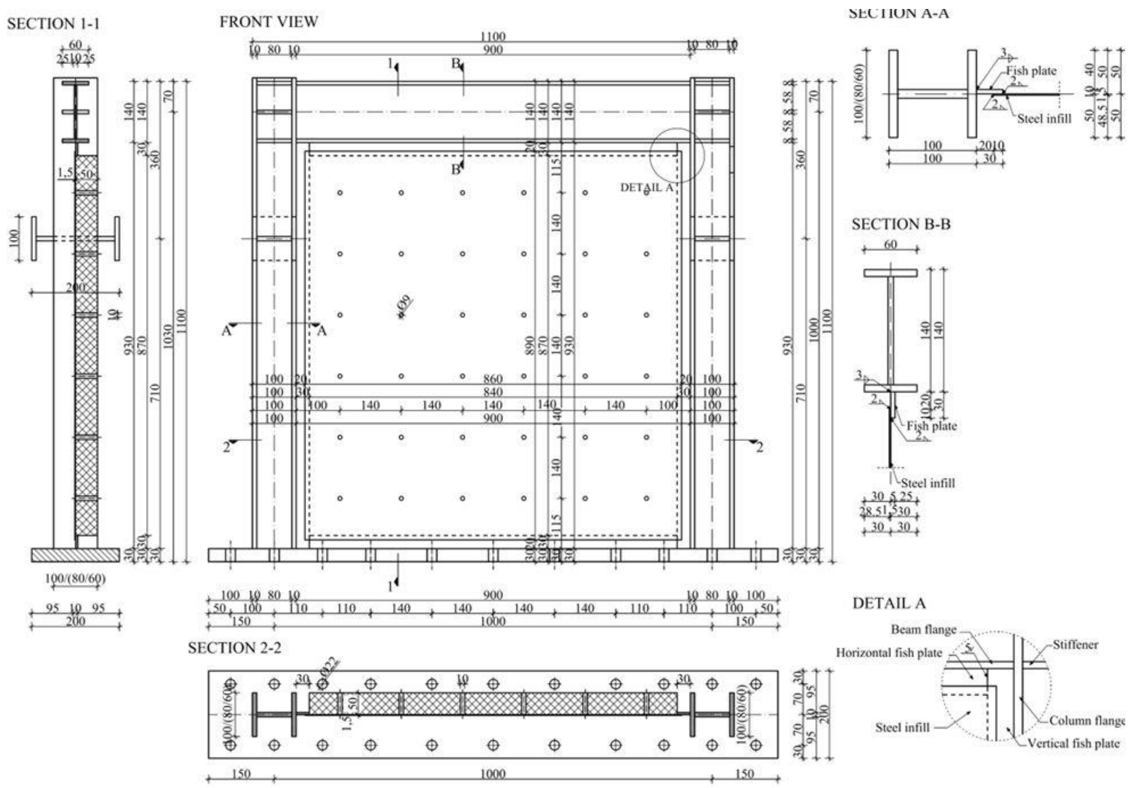

Fig. 2 CPSW specimen geometry and details (units are in mm)

conducted according to AISC 341 (AISC 2010) and CSA S16 (CSA 2009), and additional criteria found in other available literature (Qu and Bruneau 2010, Vian 2005, Park *et al*. 2007). Finally, the result was the steel part of the specimen shown in Fig. 2. On the other hand, concrete infill panel has been designed according to the requirements in EN 1998-1 (CEN 2005) and AISC 341 (AISC 2010), which mostly match each other. The result was 50 mm thick reinforced concrete panel fabricated using concrete grade C30/37 and centrally placed reinforcement mesh Q385 (Φ7 mm bars spaced at 10 cm). More details on the design procedure of the steel and concrete parts can be found in Curkovic (2017) and Curkovic *et al*. (2019).

The reference specimen (specimen label 100) was designed through the capacity design approach using 1.5 mm thick infill steel plate as a starting point. As prescribed, column cross-section of the reference specimen satisfied minimum allowed moment of inertia value, I_c, adopted in AISC 341 (AISC 2010), and CSA 16 (CSA 2009), prescribed for SPSWs. Other two specimen pairs were obtained through reduction of column flanges width, which has been done in increments 20 mm increments. Therefore, reduction of the overall column flanges width of 20 mm (specimen label 80) and 40 mm (specimen label 60) resulted with column moment of inertias that were 82% and 64% of the column moment of inertia value used for the reference specimen, respectively. In this way failure of VBEs in shear was prevented as column shear area remained almost unchanged for all tested specimens. On the other hand, design of the HBE was conducted for the most unfavourable design situation and therefore its cross-section remained unchanged for all test specimens. In order to satisfy all the design and experimental criteria, built-up I shaped cross-sections were used for all shear wall boundary elements.

Steel frames of the specimens were designed with rigid beam-to-column joints. Connection between the infill plate and the boundary elements was realized using 30x5 mm fish plates and it was continuous over the entire infill plate and fish plate perimeter, Fig. 2. Connection between steel and concrete infill panel has been designed according to Astaneh-Asl (2002) and AISC (2010). In particular, each connecting element, individually, shall be able to resist tensile force as a consequence of inelastic buckling of the steel infill plate. Additionally, connecting elements collectively shall be designed to have shear resistance greater than expected shear strength of either steel plate or reinforced concrete panel, whichever is smaller. Therefore, for the purpose of steel plate and RC panel connection, M8 8.8 steel bolts spaced at 140 mm were used. In order to obtain 1:1 specimen width-to-height aspect ratio specimens did not use foundation beam but were welded directly to the base plate which was then bolted to the reaction frame using M20 10.9 bolts with pretension. This simulated realistic situation i.e., fixed column base at the building bottom storey. Also, as foundation beams usually have high flexural stiffness, omitting them form the experiment with specimens having small column flexural stiffness would not influence the results.

Fabrication procedure concerning steel parts of the specimen has been identical to the procedure of MRF and SPSW specimen fabrication which is described in detail in Curkovic (2017) and Curkovic *et al*. (2019). As for the RC panel fabrication procedure the idea was to simulate

(a) Simulation of prefabricated RC panel (b) Ready for concrete pouring

Fig. 3 CPSW specimen

(a) RC panel side (b) Steel infill plate side

Fig. 4 CPSW specimen prepared for experimental testing

prefabricated RC panel that will, in reality, be installed after the erection of the steel part of the structure. Since the experimental specimens are scaled and the connection between steel infill plate and RC panel is predicted at 36 discrete points the possibility of error in holes positioning within the RC panel was significant. Therefore, the RC panel was fabricated directly onto the steel specimens, where steel parts of the specimens served as formwork. For that purpose, before concrete pouring, steel bolts, for connection of steel infill plates and RC panel, had to be installed and reinforcement mesh had to be placed. In order to simulate prefabricated RC panel, that would in reality have holes with diameter larger than the diameter of the connection bolt, polyvinyl chloride (PVC) tubes with outside diameter of 10 mm were placed along the bolt length, Fig. 3(a). Additionally, 3 cm thick expanded polystyrene (EPS) pieces were cut out and placed along inner flanges of boundary elements in order to form gap between RC panel and steel frame, which is common to expect when prefabricated RC panels are used. Also, such systems with gap, known as innovative CPSW systems, are expected to perform better under seismic load and should result with less damage to the RC panel, than it is common for traditional (without the gap) CPSWs (Astaneh-Asl 2002). Fig. 3(b) shows shear wall specimen prepared for concrete pouring.

After the concrete has hardened, the specimens were transported to the laboratory where final preparations before the testing were carried out. PVC tubes and EPS pieces used to assure separation between concrete and steel parts of the specimen were removed. In order to prevent fallout of the RC panel and pull-out of the bolts additional steel plates, with dimensions 30×30×5 mm, were installed on the side of the RC panel, Fig. 4(a). Finally gridlines were painted on top of the infill steel plates to have better insight of its out-of-plane deformations. After that all specimens were whitewashed in order to capture locations of nonlinear steel behaviour and to easily spot cracking of RC panel, Fig. 4(b).

3.3 Test setup and measuring devices

Loading of the specimens was conducted in vertical direction, so the specimens had to be rotated by 90° from their true position within the structure. Specimens were bolted to the supporting reaction frame which was then bolted to the strong floor. To simulate out-of-plane restraint of the CPSW due to interstorey floor structure and prevent lateral out-of-plane displacements specimens were laterally braced using lateral bracing truss. Lateral bracing truss did not provide any restraint in the in plane direction, and its position, due to actuator displacement as well as available strong floor connection points, had to be offset from the storey beam centreline to the reaction frame by 290 mm.

Fig. 5 Experimental test setup

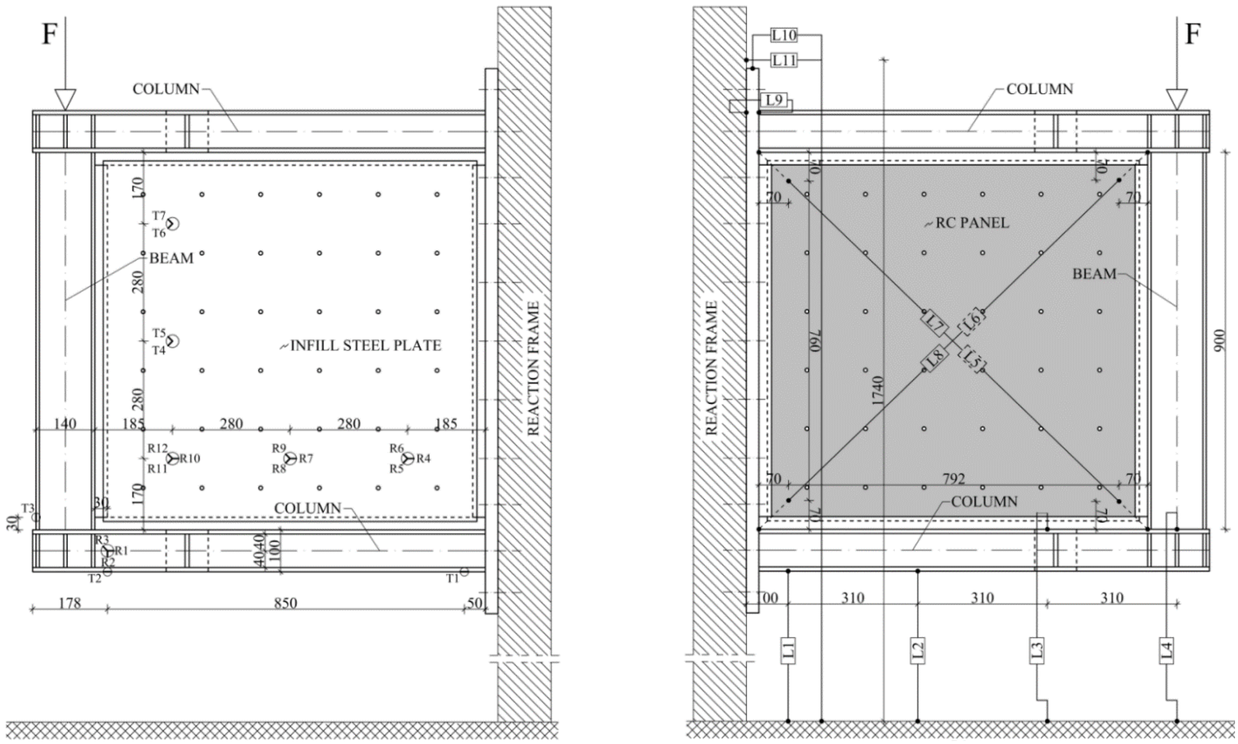

(a) Strain gauges (b) LVDT devices

Fig. 6 Position of measuring points (units are in mm)

Experimental test setup is presented in Fig. 5.

Gridlines were painted on the free side of the infill steel plate, and the specimens were afterwards whitewashed. Measuring equipment on the specimen included linear variable differential transducers (LVDT), as well as linear strain gauges and strain gauge rosettes. Detailed arrangement of all measuring devices, either LVDT or strain gauge(s), is given in Figs. 6(a)-(b), respectively. Two additional LVDT measuring devices, compared to the ones used with SPSWs in–Curkovic *et al*. (2019), have been added, namely L7 and L8, to capture change of RC panel diagonal length. To be noted is that due to the rotated testing position by 90°, Fig. 6(b), vertically measured values represent horizontal ones and vice versa. Detailed description of the other measuring points as well as test set-up can be found in Curkovic (2017) and and Curkovic *et al*. (2019).

Displacement controlled procedure has been used for the application of the loading protocol through the hydraulic actuator. The specimens were loaded with quasi-static cyclic loading and the loading protocol was defined according to ECCS (1985) and ATC-24 (1992). For the purpose of the loading protocol definition yield displacement, δ_y, had to be determined for which numerical finite element analysis of the specimen models were used according to procedure defined in Purba and Bruneau

Table 1 Mechanical properties of reinforcement steel material

Element		Proof strength at 0.2% strain	Ultimate strength	Modulus of elasticity	Elongation after fracture
		[MPa]	[MPa]	[GPa]	[%]
Φ = 7 mm	mean	523.9	586.9	174.0	2.2
	S.D.	65.1	29.3	10.7	0.3

(2014). The chosen yield displacement CPSW specimen group was 3 mm, same as for the SPSW specimens in Curkovic (2017) and Curkovic *et al*. (2019). Final definition of the loading protocol, i.e., values of the displacement amplitudes as well as the number of loading cycles per each displacement amplitude have been defined and presented in Curkovic (2017) and Curkovic *et al*. (2019). Loading of the specimens was applied at the level of the storey beam over the rigid steel adapter. The experiment was conducted up to the failure point of the specimen. Additionally, to be noted is that, due to rotated position of the test specimen, compression (C) and tension (T) in the actuator resulted in downward and upward movement of the specimen, respectively.

3.4 Material properties

Steel grade S355 was used for specimen boundary elements (6, 8 and 10 mm thick plates), while steel grade S235 was used for fish plates (5 mm thick plate), and 1.5 mm thick infill steel plate was made out of cold rolled steel DC01AM. Steel properties were determined using monotonic tensile testing according to EN ISO 6892-1 (CEN 2009).

RC panels were fabricated using concrete grade C30/37. Compressive strength was determined according to EN 12390-3 (CEN 2011) on five cubes with nominal dimension of 150 mm. Modulus of elasticity was determined according to EN 12390-13 (CEN 2013), on five cylinders with nominal diameter and height of 150 mm and 300 mm, respectively. Obtained mean value of the concrete compressive strength was 56.12 N/mm^2 with standard deviation of 0.758 N/mm^2. On the other hand, the mean value of modulus of elasticity was 30933.9 N/mm^2 with standard deviation of 582.9 N/mm^2, which is somewhat lower than the nominal value of 33000 N/mm^2.Additional information regarding mechanical properties of applied materials, as well as testing procedures can be found in Curkovic (2017) and Curkovic *et al*. (2019).

4. Experimental results and discussion

4.1 General

In order to study the influence of column flexural stiffness on the cyclic behaviour of CPSWs, the experimental program included cyclic loading of the specimens. The recorded displacement, force and strain values during each cycle of the loading protocol until the end of the experiment have been processed and afterwards used for comparison of results in terms of initial stiffness, load bearing capacity, ductility, energy dissipation capacity, damping ability, secant stiffness reduction, and column horizontal displacements profile. The testing of all specimens was carried out up to the failure point or up to the point when specimen strength dropped to about 80% value of the obtained maximum strength, either in tension or compression. The results are in most cases presented in comparison to storey drift ratio which has been calculated as the ratio of true storey displacement and storey height H (H = 1030 mm).

Also, as the prescribed column flexural stiffness requirement is identical for CPSWs and SPSWs, the results presented in this paper are compared to the results of SPSWs presented in Curkovic (2017) and Curkovic *et al*. (2017, 2019). For the purpose of the presentation and results comparison the CPSW specimens in the following are labelled as CS specimens.

4.2 Obtained results

The obtained key experimental results of specimen group CS are presented in Table 2. It is worth noting that, due to minor displacement of the steel frame carrying the actuator as well as the minor displacements of the reaction frame, the load/displacement input was not entirely symmetrical. Therefore, the results are presented separately for compression (C) and tension (T) loading direction.

The obtained results show that column moment of inertia has negligible impact on the CS specimens initial

Table 2 Key results for specimen group CS

Specimen	Initial stiffness [kN/mm]			Ultimate strength Force [kN]			Ultimate strength Displacement [mm]			Maximum displacement Force [kN]			Maximum displacement Displacement [mm]		
	(C)	(T)	mean	(C)	(T)	mean	(C)	(T)	mean	(C)	(T)	mean	(C)	(T)	mean
CS100_1	97	114	120	392	391	396	31.6	29.1	30.2	347	341	319	41.9	39.1	42.3
CS100_2	120	146		400	397		30.9	29.3		283	304		45.7	42.5	
CS80_1	97	98	104	377	374	379	31.4	29.4	30.2	271	300	279	45.3	43.0	47.1
CS80_2	97	123		383	378		30.7	29.3		274	267		51.7	48.2	
CS60_1	97	103	107	363	362	359	30.8	26.6	27.6	264	283	267	45.4	43.3	42.9
CS60_2	118	110		356	354		28.9	24.0		261	257		42.1	40.5	

(a) Without additional washer (b) With additional washer

Fig. 7 Connection detail between steel and RC plate

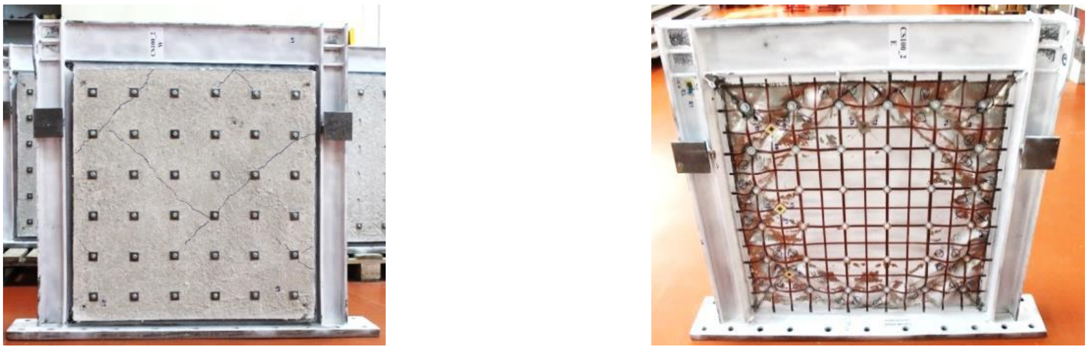

Fig. 8 Specimen CS100_2 after testing

stiffness values. As within this project experimental testing of MRF and SPSW specimens was conducted, it could be observed that initial stiffness of CS specimens is almost one order of magnitude greater and similar to the initial stiffness of MRF and SPSW specimens, respectively. As for initial stiffness, the obtained values show some inconsistencies where specimens CS80_2 and CS60_2 have higher initial stiffness than specimens with greater column flexural stiffness, i.e., specimens CS100_1 and CS80_1, respectively. These inconsistencies can be attributed to the initial imperfections and residual stresses present within the steel infill plate which might be consequence of welding on its edges, but also consequence of the fabrication errors which, when scaled specimens are used, can have significant impact on test results. Additionally, variation of the initial stiffness values can also be attributed to the small displacements of the reaction frame due to use of bolted connections between its elements, although pretension force was applied.

Expectedly, experimental results show decrease in specimen ultimate strength as a consequence of column flexural stiffness reduction. Thus, mean value of the achieved ultimate strength of the specimen pair in CS80 series is 96% (379 kN/396 kN), while of the specimen pair in series CS60 is 91% (359 kN/396 kN), of the ultimate strength mean value obtained for the specimen pair in the reference series, i.e., CS100 series.

Failure of all CS specimens started at the connections between RC panel and the steel infill plate where the bearing resistance of the infill steel plate was exceeded.

Although, this failure mode was taken into account when designing the specimens as prescribed in AISC 341 (AISC 2010) it seems that when RC panel is prefabricated and the gap between RC panel and the surrounding VBE and HBE exists, the prescribed approach is inappropriate. Such failure mode is undesirable and should be avoided for two reasons. The first reason is that, since infill steel plate failure occurred before failure of RC panel, the desired effect of energy dissipation through RC panel damaging was precluded, which resulted in somewhat pinched S-shaped hysteretic curves usually common for SPSWs. The second reason is that, due to excessive widening of the bolt hole within the infill steel plate, RC panel can fall out (out-of-plane), which presents an additional hazard, Fig. 7(a). Falling out-of-plane of RC panel happened during experimental testing of specimen CS100_1 due to which testing had to be interrupted before it was expected. Therefore, in order to carry out the experimental tests up to the failure point, to the rest of the CS specimens additional washers on the side of the infill steel plate have been added. For this purpose 3 mm thick DIN 440 R washers with outside and inside diameter of 28 mm and 9 mm, respectively, have been used, Fig. 7(b).

Further increase of loading/displacement results in development of cracks at the infill plate corners, similarly as in SPSW specimens (Curkovic *et al*. 2019), which later on propagate to the centre of the infill plate. Tension diagonals form at the infill plate corners, while the middle part of it remains almost completely intact during the entire testing, Fig. 8. Again, similarly to SPSWs, change in the load direction causes intersection of tension diagonals, which, therefore, at points where multiple plate folding occur (so called “kinks”), results in formation of cracks.

Although numerous cracks within the infill plate have

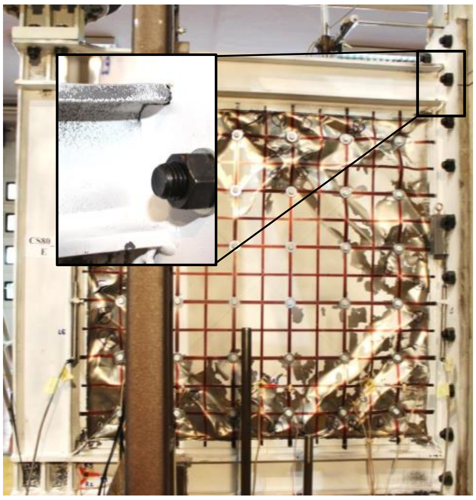

Fig. 9 Formation of the crack in HAZ and propagation into the web at load step LS18 in specimen CS80_1

been formed, failure of the specimens was reached after crack formation in the heat affected zone (HAZ) at the connection of the column outside flange and the base plate, which propagated into the column web, Fig. 9. At this point experiment was terminated. Additionally, due to failure of steel infill plate at the points of connection to the RC panel, RC panel experienced only minor diagonal cracking during the entire experiment, Fig. 8, which did not have influence on the CPSW behaviour.

4.3 Evaluation of the test results

In order to define characteristic values of the specimen behaviour, i.e., yield point, ultimate displacement, and system global ductility, actual envelope curve had to be idealised with the elastoplastic envelope curve. Idealization of the experimentally obtained envelope curve was derived using equal plastic energy concept (Curkovic *et al*. 2019). Using this procedure results in characteristic points of specimen behavior were (δ_y, V_y) defines yield point, (δ_{yi}, V_{yi}) the point of the first inelastic behaviour, and δ_{max} maximum idealised displacement of the specimen. These values were further used to calculate system global ductility value, μ_D, as δ_{max}/δ_y ratio.

Experimentally obtained cyclic envelope curves of each CS specimen are shown in Fig. 10(a), whereas calculated bilinear envelope curves and their parameters are presented in Fig. 10(b) and Table 3, respectively. Full experimental cyclic curves are shown in Fig. 13. Idealisation procedure was based on strain gauge records for which first inelastic behaviour occurred. For CS specimens critical measuring point was at steel infill plate either at measuring point Ro4 (strain gauges R10, R11 and R12) or Ro3 (strain gauges R7, R8 and R9), from the all the strain gauges placed on the steel infill plate showed also that inelastic plate buckling during the experiment has occurred, i.e., yielding of the plate occurred before it has buckled. Additionally, this confirmed that RC panel has fulfilled its main purpose which was to prevent steel infill plate elastic buckling.

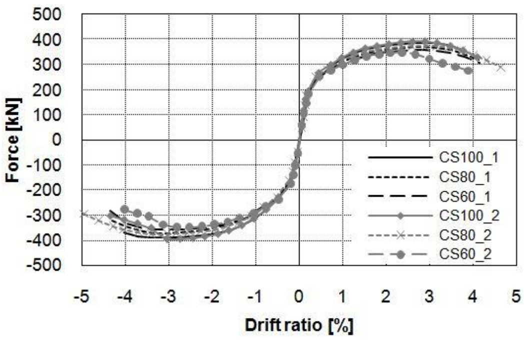

(a) Cyclic envelope curves

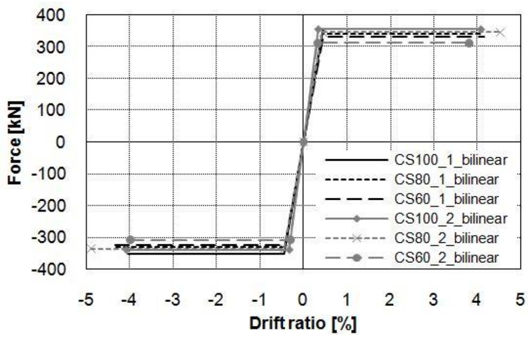

(b) Idealized bilinear envelope curves

Fig. 10 Specimen group CS curves

Table 3 Parameters of idealized bilinear curves for CS specimen group

Specimen	Initiation of inelastic behaviour				Yield point				Ultimate displacement		Ductility	
	V_{yi} [kN]	δ_{yi} [mm]	Direction	Critical location	V_y [kN] (C)	V_y [kN] (T)	δ_y [mm] (C)	δ_y [mm] (T)	δ_{ult} [mm] (C)	δ_{ult} [mm] (T)	μ_D (C)	μ_D (T)
CS100_1	154	2.0	(C)	Ro4	352	357	4.6	4.6	41.5	38.7	9.0	8.4
CS100_2	193	1.9	(T)	Ro3	340	356	3.3	3.5	42.0	42.1	12.7	12.0
CS80_1	156	2	(C)	Ro4	333	342	4.3	4.4	44.4	42.4	10.3	9.6
CS80_2	120	1.6	(C)	Ro4	337	346	4.5	4.6	50.3	46.6	11.2	10.1
CS60_1	183	2.5	(C)	Ro4	326	332	4.5	4.5	44.6	42.7	9.9	9.5
CS60_2	125	1.3	(C)	Ro4	309	312	3.2	3.2	41.1	39.2	12.8	12.3

Behaviour of specimens under cyclic loading was also evaluated through secant stiffness reductions. Average secant stiffness, K_{isec}, was determined separately for tension and compression loading, and for each loading step. The value of the average secant stiffness for the i-th loading step was calculated as

$$K_i^{\sec} = \frac{\sum_n V_i^n}{\sum_n \delta_i^n} \quad (i = 1, 2,..., m) \text{ and } (n = 2 \text{ or } 3) \tag{3}$$

where δ_{in} is the highest displacement in tension or compression of n-th cycle of the i-th load step, while V_{in} is the corresponding horizontal force at storey height. The calculated secant stiffness values are presented in Fig. 11.

It can be seen all CS specimens show stable secant stiffness reduction throughout entire duration of the experiment. Variation of the initial values of the specimen stiffness was explained earlier in the text, and it did not have any impact on the overall behaviour of the specimens. The obtained results confirm stable and acceptable behaviour up to 4% storey drift ratios of all CS specimens that were tested, even for the ones whose column flexural stiffness did not satisfy minimum prescribed value.

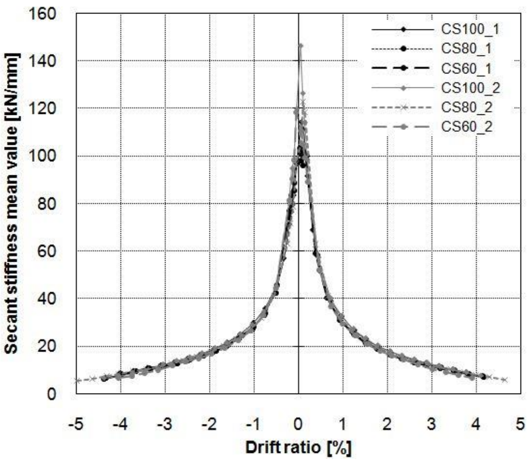

Fig. 11 Specimen group F secant stiffness reduction

In order to obtain horizontal displacement profiles of columns, displacements of columns were measured at four points (LVDT L1 to L4), Fig. 6(b). Column horizontal displacement profiles are presented for two different storey drifts, namely 2.5% and 4%, in Figs. 12(a)-(b), respectively. Results of CS specimens show small amount of column "pull-in" deformation at the measuring point L1, and show virtually no difference of the "pull-in" deformation regardless of the column flexural stiffness value used. On the other hand, all specimens had stable secant stiffness reduction, thus indicating that the measured "pull-in" deformation has no negative impact on the overall CSPW behaviour. Therefore it can be concluded that the prescribed column flexural stiffness requirement might be excessively conservative; additionally, as the horizontal displacement profiles of all the CS specimens almost coincide, the results also indicate that the prescribed requirement might also be completely unnecessary.

4.4 Comparison of results between CPSWs and SPSWs

As the design of CPSWs is mostly based on the assumptions derived for SPSWs, the experimentally obtained results for the two stabilization systems are compared each other. Additionally, the results of the tested MRF have also been included in the comparison procedure. Detailed experimental results of MRFs and SPSWs, labelled here as results of specimen group F and S, respectively, can be found in Curkovic (2017) and Curkovic *et al*. (2019).

Resume of the experimental results mean values for specimens of F, S and CS group is given in Table 4. Comparing the results it can be seen that RC panel has increased initial stiffness value, i.e., by approximately 25% (110/88 kN/mm). It is important to mention that the initial stiffness results had great variation, due to use of small scaled specimens and it is probable that such high increase of initial stiffness value between SPSW and CPSW specimens might be unrealistic, especially since innovative CPSW (with the gap around RC panel) have been used.

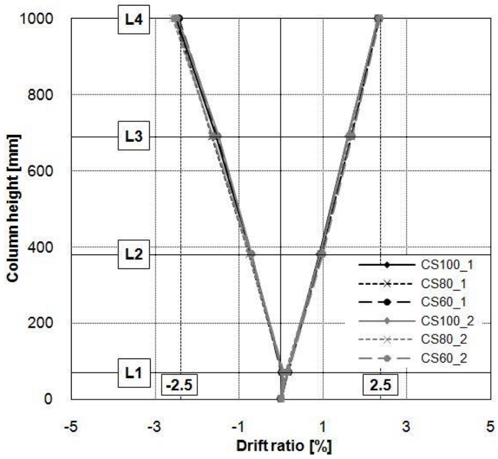

(a) 2.5% drift

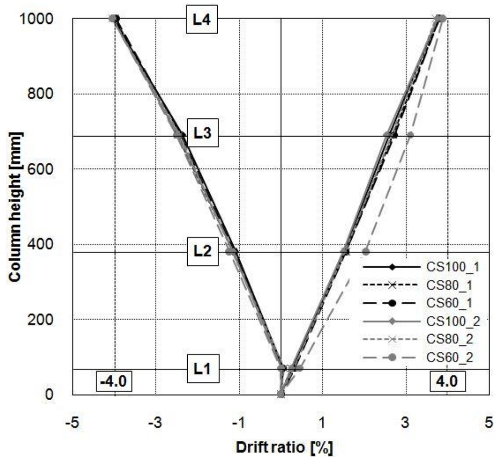

(b) 4% drift

Fig. 12 Column horizontal displacement profiles for CS specimen group

Table 4 Resume of the experimental results mean values for F, S and CS specimen groups

Specimen	Initial stiffness [kN/mm]	Ultimate strength [kN]	Ductility [-]
F100	13.7	208	5.3
F80	12.3	178	6.1
F60	10.7	137	5.0
S100	100	371	11.1
S80	75	342	9.6
S60	89	321	17.0
CS100	120	396	10.5
CS80	104	379	10.3
CS60	107	359	11.1

Also, application of the RC panel to SPSWs has increased CS specimen ultimate strength for approximately 10%. Since in CPSW infill steel plate participates to the greater extent in the bearing resistance of CPSWs than is the case in SPSW, the change of column flexural stiffness has even lower impact on the ultimate strength. Furthermore, the mean value of the difference between ultimate strength of CS and F specimens was calculated and amounts to 203 kN. Similar difference can be calculated for S and F specimens, where it amounts to 170 kN. This indicates that infill steel plate strength has, due to RC panel application, increased by 19% (203/170 kN). On the other hand, if the mean value of the infill steel plate strength is calculated using (1) and experimentally obtained steel material ultimate strength value from Curkovic (2017) and Curkovic *et al.* (2019), the value of 250 kN is obtained. This result leads to conclusion that infill steel plate has not completely yielded in shear, as is expected for CPSWs, but some parts of it started buckling before yielding. This is in accordance with the observations during the experiment where, due to failure of the infill steel plate around the connections to the RC panel, the steel infill was not supported in the out-of-plane direction anymore. Finally, it can be observed that implementation of RC panel to SPSW has negligible impact on the reduction of CPSW system global ductility.

Experimentally obtained hysteretic curves with corresponding envelope curves of S and CS specimen groups are shown in Fig. 13. CS specimens show less pinching in the II and IV quadrant due to application of RC panel which prevents buckling of the steel infill plate and therefore allows for transfer of compression stresses. However, hysteretic curves did show more pinching than usual for CPSWs which is attributed to the unwanted bearing resistance failure of the steel infill plate at the connections to the RC panel. Such failure mode prevented

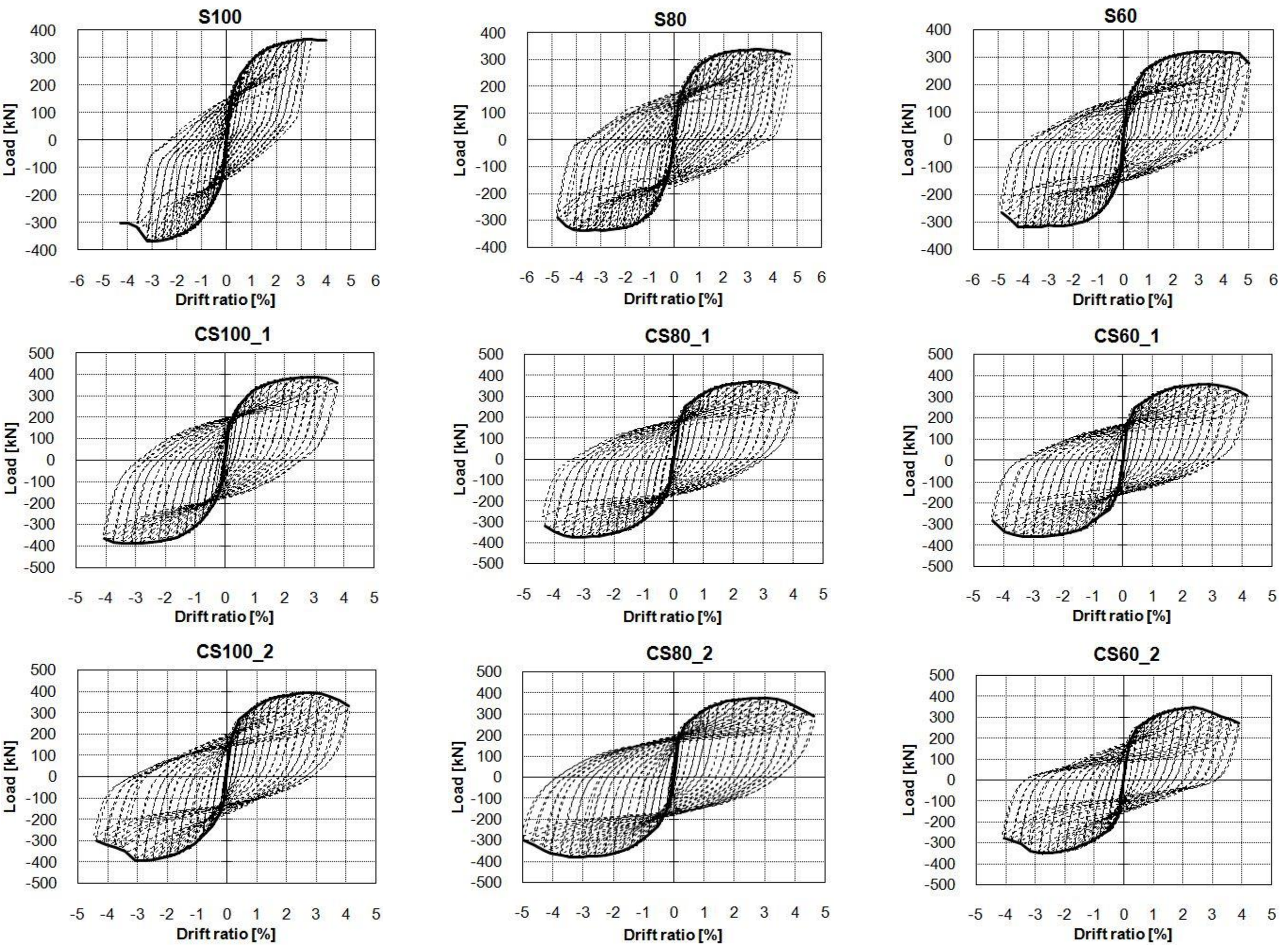

Fig. 13 Comparison of hysteretic curves and corresponding envelope curves

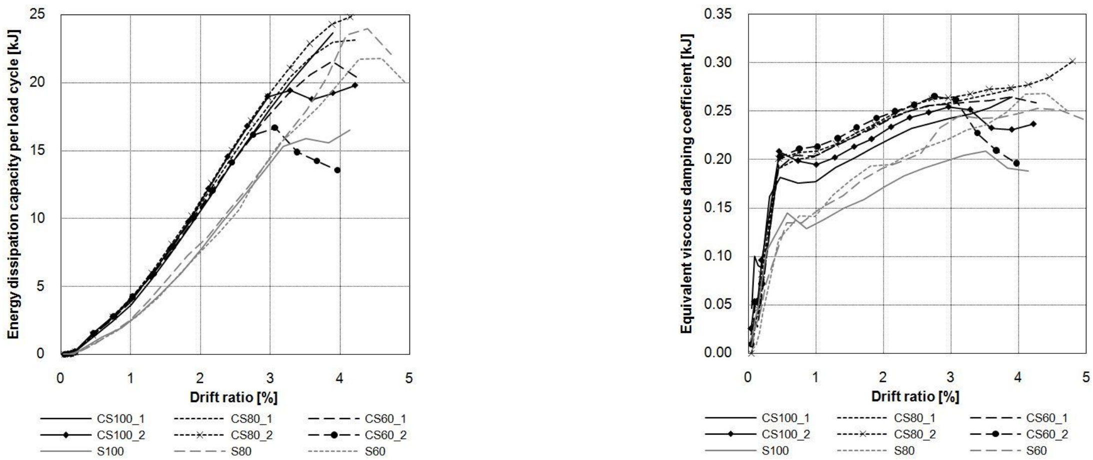

(a) Energy dissipation capacity (b) Equivalent viscous damping coefficient

Fig. 14 Comparison of experimental values of S and CS specimens

dissipation of the energy that was supposed to occur within the RC panel through its cracking.

For the purpose of quantitative comparison of CS and S specimen groups, energy dissipation capacity as well as equivalent viscous damping coefficient can be calculated from the experimentally obtained hysteretic curves. These values per load cycle of each load step for all the specimens are compared in Figs. 14(a)-(b), respectively. Again, even though early exceedance of the steel infill plate bearing resistance precluded desired behaviour of the CS specimen group, where instead of the steel infill plate the RC panel should sustain larger damage, the CPSW specimens did allow for larger energy dissipation during the entire experiment, Fig. 14(a). Also, as presented in Fig. 14(b), during the entire experiment the value of equivalent viscous damping coefficient of CPSWs appears to be greater than of the SPSWs. Finally, it should be observed that the obtained equivalent viscous damping curves are qualitatively similar indicating that the inelastic behaviour in CPSW and SPSW occurs at approximately the same drift ratios.

5. Development and validation of finite element model

5.1 General

Before the experimental tests, finite element models of the specimens were developed using commercially available finite element software Ansys 14.5 (ANSYS 2012). Those FE models did not include simulation of the RC panel and they served for the purpose of determination of the yield displacement, δ_y, which was necessary to define the loading protocol to be used during the experimental testing. Modelling of RC panel was avoided as it was expected that it would not significantly influence the yield displacement determined for the SPSWs, and also for the reason that the same cyclic loading protocol was to be used with SPSW and CPSW specimens during the experiment. After the experimental investigation, the FE models were calibrated using the results and observations collected during the experimental tests. Calibration of FE models was necessary in order to obtain reliable models needed for further parametric numerical analyses.

5.2 Modelling assumptions

Three dimensional models using static structural analysis module in Workbench, which uses implicit solving methods, were created in Ansys 14.5 (ANSYS 2012). Due to complexity of the problem that was to be simulated the balance was sought between the finite elements selection and the available resources (time and computational resources). Therefore, 4-node shell elements SHELL 181 were chosen to simulate all the steel parts of the tested specimens (frame elements and infill plates), while 8-node solid elements SOLID65 were used to simulate RC panels. Shell finite elements allowed for simulation of complex stress distribution present within the steel parts, and also enabled simulation of initial imperfections of the steel plate. On the other hand, solid finite elements allowed simulation of concrete plastic deformation, cracking in tension in three orthogonal directions, and crushing of concrete in compression. Also, these FE elements allowed for simulation of reinforcement bars as the percentage of the total element volume, where the reinforcement percentage can be defined separately for three different directions. For the simulation of the connection between steel infill plate and RC panel, i.e., steel bolts, 2-node beam elements BEAM188 were used, Fig. 15. Nodes of these finite elements were connected to the coincident nodes of shell and solid elements by coupling their degrees of freedom. As SOLID65 elements only have translational degrees of freedom and in reality steel bolts are not prevented to rotate about its longitudinal axis, such simulation of coupled connection is accurate. In order to reduce complexity of the model, other connections, i.e., connections between steel infill plate and the boundary frame, as well as the beam-to-column connections were avoided in those nodes between these elements were shared.

The reaction frame, out-of-plane support, base plate as well as rigid adapter for the force/displacement input have

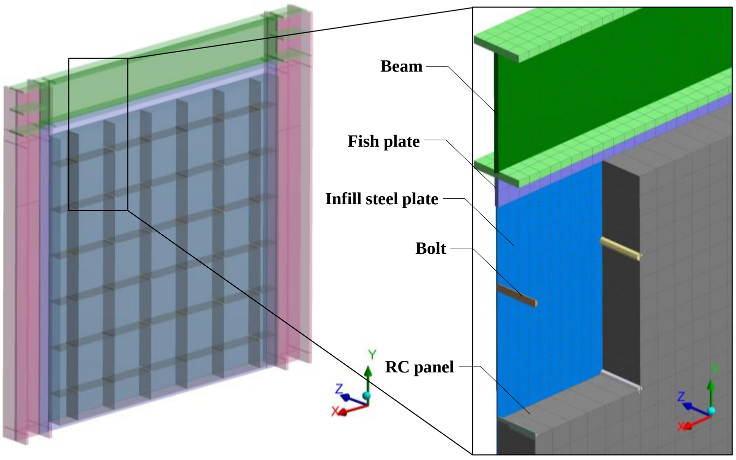

Fig. 15 FE simulations of the discrete connection and contact between steel and RC plate

not been modelled in order to reduce FE model complexity. Instead, fixed support preventing all six degrees of freedom was used to simulate connection of the columns and bottom fish plate to the base plate, while prevention of displacement only in global Z direction simulated out-of-plane support. Displacement input was conducted over number of edges in order to simulate rigid adapter used during the experiment. Finally, contacts were defined between steel infill plate and the RC panel, as shown in Fig. 15. For that purpose frictionless contact type was defined, which allowed formation of the gaps between the bodies and their free sliding, but prevented penetration of one body into the other. Finite element models were tested under monotonic loading, i.e., pushover analyses for both load directions were conducted. Simulated boundary conditions are presented in Fig. 16. Simulation of the initial imperfection, as was the case for SPSW (Curkovic *et al*. 2019), was avoided with the CPSW FE model. Namely, the CPSW FE models, unlike SPSW FE models, were not symmetrical about their plane so buckling of the steel infill plate would eventually occur during the analysis, therefore precluding excessive rigidity of the model and providing reliable results.

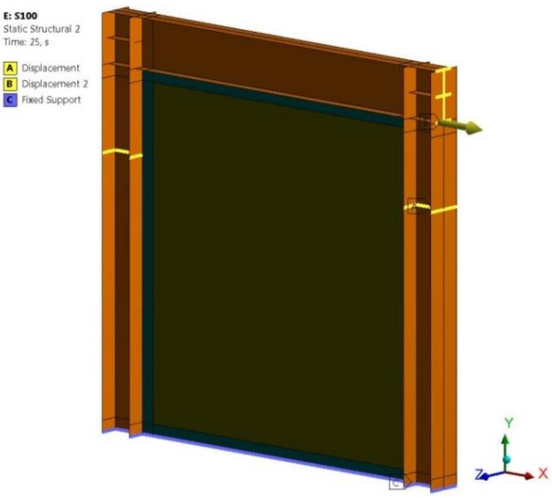

Fig. 16 FE simulations of boundary conditions

5.3 Material models

Properties of the steel material have been determined using standard tensile test of the steel probes, and the obtained results are given in Curkovic (2017) and Curkovic *et al*. (2019). Since steel material under monotonic and cyclic load behaves differently the material stress-strain curves used in FE simulations were determined from the monotonic results using approach proposed by Budahazy (2015). However, cyclic strass-strain curves were used for all steel materials except for the steel material of the infill panel. This was due to fact that infill panel presents very slender element which can only carry negligible amount of compression force and would not therefore experience cyclic loading in tension and compression. Additionally, the proposed approach was slightly modified omitting isotropic hardening and taking into account only kinematic hardening of the material. Furthermore, failure of the steel material has not been simulated. Finally, steel material of the bolts has not been experimentally tested, and therefore nominal values were used within the simulation.

The experimentally obtained results for the concrete, given in subsection 3.2, have been used to define constitutive law for the concrete material in compression as well as in tension. Behaviour of concrete in compression, before the cracking occurs, was defined using multilinear isotropic constitutive model. The multilinear isotropic concrete model uses von Mises yield criteria along with

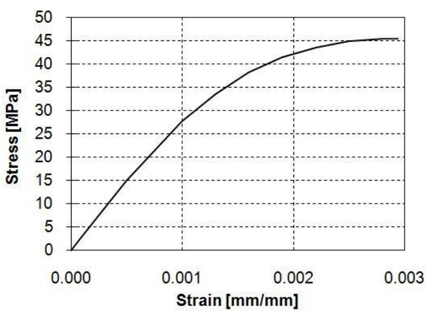

Fig. 17 Stress-strain curve of concrete under monotonic compressive load

Willam and Warnke model (Willam and Warnke 1975), in order to define failure of concrete. The compressive uniaxial stress-strain relationship of the concrete model presented in Fig. 17 was obtained using following expressions according to Desayi and Krishnan (1964)

$$\sigma = \frac{E_c \, \varepsilon}{1 + \left(\dfrac{\varepsilon}{\varepsilon_0} \right)^2}, \tag{4}$$

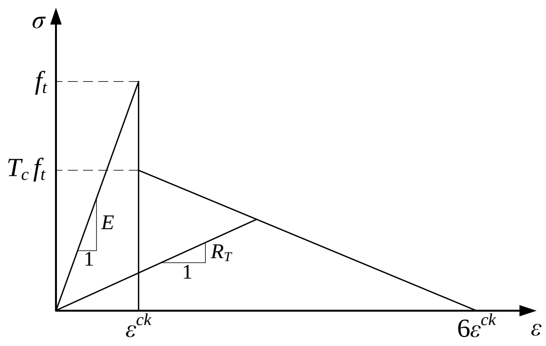

Fig. 18 Strength of cracked condition (ANSYS 2012)

$$\varepsilon_0 = \frac{2 \, f_c}{E_c}, \tag{5}$$

where σ is stress at any strain value, ε is strain at stress σ, ε_0 is strain at ultimate compressive strength, f_c is uniaxial ultimate concrete compressive strength, and E_c is concrete modulus of elasticity.

Even though the applied concrete material model was able to simulate failure of concrete in compression and its behaviour after the failure this option was avoided in the modelling of the CPSW since no concrete crushing was observed during the experimental testing. Additionally, to define the concrete constitutive law compressive cylinder strength of concrete was needed but during the experiment only the compressive cube strength of concrete was determined. Therefore, the characteristic compressive cylinder strength was determined as f_{ck} = 0,8 $f_{ck,cube}$. Behaviour of concrete in tension was defined as linear elastic using again the experimentally obtained modulus of elasticity, after which failure occurs. When the failure surface is reached stresses have sudden drop in that direction. In order to achieve convergence strain softening has been applied, where the stresses after a failure drop to a 60% value of the concrete tensile strength and afterwards gradually drop to zero, Fig. 18. In order to consider

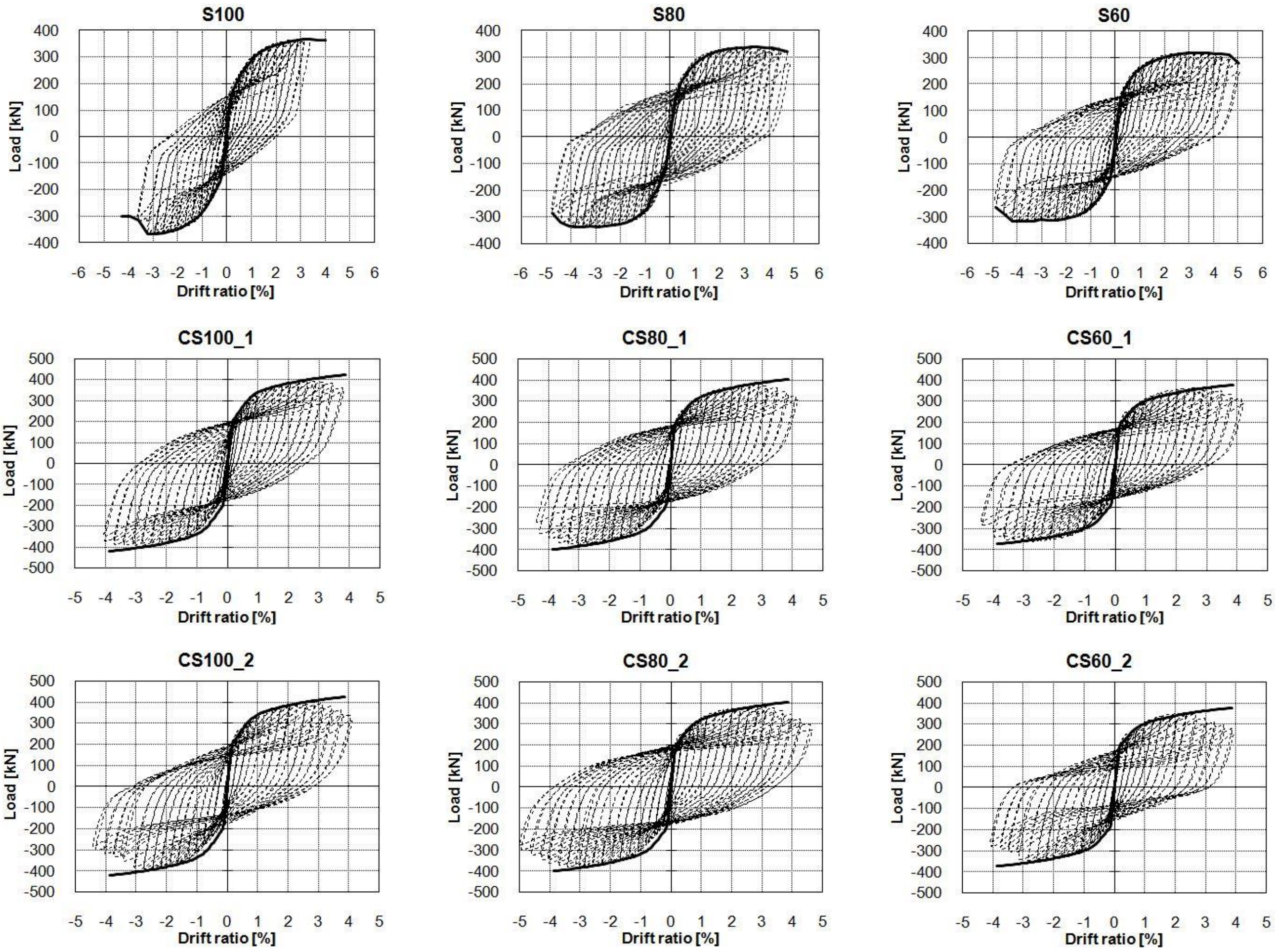

Fig. 19 Comparison of experimental hysteretic curves with corresponding FE pushover curves

retention of shear stiffness in cracked concrete two shear transfer coefficients have been defined. One coefficient for open cracks with the value of 0.15, and the other for closed cracks with the value of 0.4. Finally, as the concrete tensile strength has not been experimentally determined it was derived using expression (6) provided in fib 2010 (fib 2013), which is valid for concrete grades lower than C50.

$$f_{ctm} = 0{,}3\left(f_{ck}\right)^{2/3} \tag{6}$$

The steel reinforcement was modelled using smeared concept, where the reinforcement is modelled as some percentage of the finite element volume used to simulate concrete matrix. Therefore, for each in-plane orthogonal direction the reinforcement was modelled with volume ratio of 0,8%. Reinforcement steel uses bilinear elastoplastic constitutive model with kinematic hardening, where the values of the elasticity modulus and yield strength were taken as experimentally determined while the hardening modulus was taken as 1% of the determined elasticity modulus value. Generally, more details on all material models can be found in Curkovic (2017).

5.4 Results and FE model validation

The experimentally obtained hysteretic force-displacement curves were compared to the FE pushover curves for each loading direction. Since failure of the test specimen occurred due to crack formation at the column bottom and steel material failure has not been modelled it is obvious that such failure mechanism cannot be properly simulated. But simulations are expected to correlate well up to the point of crack opening which in the experimental testing never occurred before 2.5% storey drift ratio which is assumed to be the ultimate displacement limit according to EN 1998-1 (CEN 2004).

The comparison of FE pushover curves in tension and compression with experimentally obtained hysteretic curves for specimen group CS are shown in Fig 19. Graphically results seem to compare well, but for more detailed analysis results are compared regarding initial stiffness values as well as realized strength at 2.5% storey drift ratio. For that purpose percentage of error of numerical to experimental value was calculated using the following expression

$$ERR. = \frac{FEM. - EXP.}{EXP.}, \tag{7}$$

where *FEM.* indicates mean value for results of numerical analysis, while *EXP.* indicates mean value obtained for results of experimental analysis. Percentage of error can have negative or positive value if numerically obtained result is lower or higher than experimentally obtained result, respectively.

Experimental and numerical results of all tested specimens are given in Table 5. Numerical results at 2.5% drift ratio show good agreement regarding the amount of realized horizontal load. As can be seen the highest strength deviations are obtained for specimen CS80_1 where numerical value exceeds the experimental result by 1.7%.

Table 5 Comparison of experimental and numerical strength and initial stiffness

Specimen	Load at ±2.5% drift ratio			Initial stiffness		
	[kN]		[%]	[kN/mm]		[%]
	EXP.	*FEM.*	*ERR.*	*EXP.*	*FEM.*	*ERR.*
CS100_1	384.6	391.0	1.6	97.5	166.7	71.9
CS100_2	390.9		0.0	119.8		38.9
CS80_1	367.9	374.3	1.7	96.9	161.4	66.4
CS80_2	372.8		0.4	96.7		66.4
CS60_1	357.1	352.6	-1.3	97.0	155.5	60.3
CS60_2	348.2		1.3	118.1		31.8

On the other hand, numerical values of the initial stiffness show large deviation, where the most unfavourable value is obtained for specimen CS100_1 whose numerical initial stiffness value is 71.9% higher than the experimentally obtained value. It is also to be noted that numerical values compared to the experimental ones, for the same specimen pair, also show large deviations. This is partially attributed to avoidance of modelling of the infill steel plate initial imperfections which inevitably increased initial stiffness of the CPSW models. Therefore these FE models are not suitable for determination of the CPSW initial stiffness. As can be seen initial stiffness deviations did not influence other FE results which compare well to the experimental ones.

Finally, these numerical simulations did not include cyclic loading of the specimens and thus are not acceptable for comparison with experimentally obtained column displacement profiles. For that purpose refined FE simulations including cyclic loading should be developed.

6. Conclusions

In this paper experimental and numerical analyses on Composite (steel-concrete) Plate Shear Walls with different column moment inertia values were conducted in order to investigate the impact of various column flexural stiffness on the overall performance of CPSW systems subjected to cyclic lateral loads. For this purpose, three pairs of one-storey one-bay CPSW specimens were designed, fabricated and tested. In order to fulfil strength requirements, boundary elements were designed using capacity approach. The variation of column flexural stiffness was achieved through the reduction of column flanges width. As the requirement for the minimum allowed column flexural stiffness is overtaken from indications available for simple Steel Plate Shear Walls, the experimental results of CPSWs and SPSWs were compared. In addition, two different finite element models were developed during the investigation. The first model served to determine the yield displacement necessary to define experimental loading protocol. In that model experimentally obtained steel material data was applied. The second model was modified based on experimental results and observations. Based on the obtained experimental and numerical results the following main outcomes have been determined:

- initial stiffness of CPSWs is to the greatest extent influenced by the steel infill panel and only to a lesser extent by the RC panel; in fact, comparing the initial stiffness between SPSWs and MRFs the difference is almost 1000%, while between CPSWs and SPSWs it is only from 10 to 20%;
- column flexural stiffness reduction of 36% did not impact CPSW system cyclic ductility, as all tested specimens tolerated story drift ratios up to 4%;
- all CPSW specimens showed stable secant stiffness reduction throughout the entire experiment even though the minimum flexural stiffness requirements of surrounding columns were not satisfied;
- insignificant "pull-in" deformation of VBEs near their base connection was observed even for storey drift ratios of 4%;
- "pull-in" deformation of the VBEs recorded for the CPSWs was lower than "pull-in" deformation within SPSWs; this confirms more favourable stress state acting on the VBEs of CPSWs than of SPSWs;
- "pull-in" of the VBEs did not have negative impact on the overall CPSW system behaviour; this is clearly visible from stable secant stiffness reduction, as well as from energy dissipation and damping capacity diagrams;
- although RC panel enabled inelastic steel infill plate buckling, premature exceedance of the steel infill plate bearing resistance at the connections to the RC panel precluded steel infill plate yielding in shear; as a consequence, the proposed procedure for the design of the connection should be revised, particularly if precast RC concrete panels are used;
- developed FE models can reasonably predict experimentally obtained behaviour of CPSWs and can be used for the purpose of numerical parametric analyses; additionally, to enable reliable prediction of the specimen initial stiffness steel infill plate initial imperfections need to be simulated.

As a main general conclusion, it is worth noticing that this research has indicated that current requirement for column flexural stiffness used for SPWSs might be conservative in case of CPSW systems. For that purpose further investigation applying either experimental or numerical research methods should be conducted.

References

AISC (2010), ANSI/AISC 341-10: Seismic Provisions for Structural Steel Buildings; American Institute of Steel Construction (AISC), Chicago, IL, USA.

Ali, M.M., Osman, S.A., Husam, O.A. and Al-Zand, A.W. (2018), "Numerical study of the cyclic behavior of steel plate shear wall systems (SPSWs) with differently shaped openings", *Steel Compos. Struct., Int. J.*, **26**(3), 361-373. https://doi.org/10.12989/scs.2018.26.3.361

ANSYS (2012), User's Manual (Version 14.5); Swanson Analysis Systems Inc., Houston, TX, USA.

Arabzadeh, A., Soltani, M. and Ayazi, A. (2011), "Experimental investigation of composite shear walls under shear loadings", *Thin-Wall. Struct.*, **49**(7), 842-854. https://doi.org/10.1016/j.tws.2011.02.009

Astaneh-Asl, A. (2002), *Seismic Behavior and Design of Composite Steel Plate Shear Walls*, Steel TIPS Report, Structural Steel Education Council, Moraga, CA, USA.

ATC (1992), ATC-24: Guidelines for Cyclic Seismic Testing of Components of Steel Structures; Applied Technology Council, Redwood City, CA, USA.

Brando, G., D'Agostino, F. and De Matteis, G. (2013), "Experimental tests of a new hysteretic damper made of buckling inhibited shear panels", *Mater. Struct./Materiaux et Constructions*, **46**, 2121-2133. https://doi.org/10.1617/s11527-013-0040-6

Budahazy, V. (2015), "Uniaxial cyclic steel behavior and model for dissipative structures", Ph.D. Dissertation; Budapest University of Technology and Economics, Budapest, Hungary.

CEN (2004), EN 1998-1: Eurocode 8. Design of structures for earthquake resistance – Part 1: General rules, seismic actions and rules for buildings; European Committee for Standardization, Brussels, Belgium.

CEN (2005), EN 1993-1-1: Eurocode 3: Design of steel structures – Part 1-1: General rules and rules for buildings; European Committee for Standardization, Brussels, Belgium.

CEN (2009), EN ISO 6892-1:2009 – Metallic materials – Tensile testing – Part 1: Method of test at room temperature; European Committee for Standardization, Brussels, Belgium.

CEN (2011), EN 12390-3:2009 – Testing hardened concrete - Part 3: Compressive strength of test specimens; European Committee for Standardization, Brussels, Belgium.

CEN (2013), EN 12390-13:2013 – Testing hardened concrete - Part 13: Determination of secant modulus of elasticity in compression; European Committee for Standardization, Brussels, Belgium.

CSA (2009), S16-09 Design of Steel Structures; Canadian Standards Association, Toronto, ON, Canada.

Curkovic, I. (2017), "Behaviour of composite plate shear walls under earthquake", Ph.D. Dissertation; University of Zagreb, Zagreb, Croatia. [In Croatian]

Curkovic, I. and Dzeba, I. (2016), "State of the art review on behaviour and calculation of composite plate shear walls", *Tehnicki Vjesnik-Technical Gazette*, **23**(5) 1523-1532. https://doi.org/10.17559/TV-20141111103014

Curkovic, I., Skejic, D. and Dzeba, I. (2017), "11.24: Impact of column flexural stiffness on behaviour of steel plate shear walls", *ce/papers*, **1**(2-3), 3023-3032. https://doi.org/10.1002/cepa.354

Curkovic, I., Skejic, D. and Dzeba, I. (2019), "Seismic performance of steel plate shear walls with variable column flexural stiffness", *Steel Compos. Struct., Int. J.*, **33**(1), 833-850. https://doi.org/10.12989/scs.2019.33.1.833

De Matteis, G., Landolfo, R. and Mazzolani, F.M. (2003), "Seismic response of MR steel frames with low-yield steel shear panels", *Eng. Struct.*, **25**(2), 155-168. https://doi.org/10.1016/S0141-0296(02)00124-4

De Matteis, G., Mazzolani, F.M. and Panico, S. (2007), "Pure aluminium shear panels as dissipative devices in moment-resisting steel frames", *Earthq. Eng. Struct. Dyn.*, **36**, 841-859. https://doi.org/10.1002/eqe.656

De Matteis, G., Mazzolani, F.M. and Panico, S. (2008), "Experimental tests on pure aluminium shear panels with welded stiffeners", *Eng. Struct.*, **30**(6), 1734-1744. https://doi.org/10.1016/j.engstruct.2007.11.015

De Matteis, G., Sarracco, G. and Brando, G. (2016), "Experimental tests and optimization rules for steel perforated shear panels", *J. Constr. Steel Res.*, **12**, 41-52. https://doi.org/10.1016/j.jcsr.2016.04.025

Desayi, P. and Krishnan, S. (1964), "Equation for the stress-strain

curve of concrete", *ACI Journal*, **61**(3), 345-350.
Driver, R.G., Kulak, G.L., Kennedy, J.L. and Elwi, A.E. (1998), "Cyclic test of four-story steel plate shear wall", *ASCE, J. Struct. Eng.*, **124**(2), 112-120. https://doi.org/10.1061/(ASCE)0733-9445(1998)124:2(112)
ECCS (1985), Recommended Testing Procedures for Assessing the Behavior of Structural Elements Under Cyclic Loads; European Convention for Constructional Steelwork, Technical Committee 1, TWG 1.3 – Seismic Design, No. 45, Brussels, Belgium.
Elgaaly, M., Caccese, V. and Du, C. (1993), "Postbuckling behavior of steel plate shear walls under cyclic loads", *ASCE, J. Struct. Eng.*, **119**(2), 588-605. https://doi.org/10.1061/(ASCE)0733-9445(1993)119:2(588)
fib (2013), fib Model Code for Concrete Structures 2010; Wilhelm Ernst & Sohn, Berlin, Germany.
Guo, L., Rong, Q., Qu, B. and Liu, J. (2017), "Testing of steel plate shear walls with composite columns and infill plates connected to beams only", *Eng. Struct.*, **136**, 165-179. https://doi.org/10.1016/j.engstruct.2017.01.027
Hadzhiyaneva, I. and Belev, B. (2014), "Behaviour of Steel Plate Shear Walls with Buckling-Restrained Web Panels", *Proceedings of Second European Conference on Earthquake Engineering and Seisimology*, Istanbul, Turkey, August.
Hou, H., Qiu, C., Lv, Z. and Sun, Y. (2013), "Cyclic behavior of steel frames infilled with composite panels: experimental and numerical", *Open Civil Eng. J.*, **7**, 196-204.
ISO (2010), ISO 15630-1:2010 – Steel for the reinforcement and prestressing of concrete – Test methods – Part 1: Reinforcing bars, wire rod and wire; International Organization for Standardization, Geneva, Switzerland.
Jin, S., Ou, J. and Liew, J.Y.R. (2016), "Stability of buckling-restrained steel plate shear walls with inclined-slots: theoretical analysis and design recommendations", *J. Constr. Steel Res.*, **117**, 13-23. https://doi.org/10.1016/j.jcsr.2015.10.002
Kalali, H., Hajsadeghi, M., Zirakian, T. and Alaee, F.J. (2015), "Hysteretic performance of SPSWs with trapezoidally horizontal corrugated web-plates", *Steel Compos. Struct., Int. J.*, **19**(2), 277-292. https://doi.org/10.12989/scs.2015.19.2.277
Kuhn, P., Peterson, J.P. and Levin, L.R. (1952), *A Summary of Diagonal Tension Part I: Methods and Analysis, Technical Note 2661*, National Advisory Committee for Aeronautics, Washington, D.C., USA.
Li, C.H., Tsai, K.C. and Lee, H.C. (2014), "Seismic design and testing of the bottom vertical boundary elements in steel plate shear walls. Part 2: experimental studies", *Earthq. Eng. Struct. Dyn.*, **43**, 2155-2177. https://doi.org/10.1002/eqe.2442
Lie, W.-Y., Li, G.-Q. and Jiang, J. (2018), "Experimental study on reinforced concrete frames with two-side connected buckling-restrained steel plate shear walls", *Adv. Struct. Eng.*, **21**(3), 460-473. https://doi.org/10.1177/1369433217719985
Liu, W.-Y., Li, G.-Q. and Jiang, J. (2017), "Mechanical behavior of buckling restrained steel plate shear walls with two-side connections", *Eng. Struct.*, **138**, 283-292. https://doi.org/10.1016/j.engstruct.2017.02.010
Lubell, A.S., Prion, H.G.L., Ventura, C.E. and Rezai, M. (2000), "Unstiffened steel plate shear wall performance under cyclic loading", *ASCE J. Struct. Eng.*, **126**(4), 453-460. https://doi.org/10.1061/(ASCE)0733-9445(2000)126:4(453)
Machaly, E.B., Safar, S.S. and Amer, M.A. (2014), "umerical investigation on ultimate shear strength of steel plate shear walls", *Thin-Wall. Struct.*, **84**, 78-90. https://doi.org/10.1016/j.tws.2014.05.013
Massumi, A., Karimi, N. and Ahmadi, M. (2018), "Effects of openings geometry and relative area on seismic performance of steel shear walls", *Steel Compos. Struct., Int. J.*, **28**(5), 617-628. https://doi.org/10.12989/scs.2018.28.5.617
Montgomery, C.J. and Medhekar, M. (2001), "Unstiffened steel plate shear wall performance under cyclic loading", *ASCE J. Struct. Eng.*, **127**(8), 973-975. https://doi.org/10.1061/(ASCE)0733-9445(2001)127:8(973)
Qi, Y., Gu, Q., Sun, G. and Zhao, B. (2017), "Shear force demand on headed stud for the design of composite steel plate shear wall", *Eng. Struct.*, **148**, 780-792. https://doi.org/10.1016/j.engstruct.2017.07.023
Qu, B. and Bruneau, M. (2010), "Behaviour of vertical boundary elements in steel plate shear walls", *Eng. J.*, **47**, 109-122.
Park, H.G., Kwack, J.H., Jeon, S.W., Kim, W.K. and Choi, I.R. (2007), "Framed steel plate wall behavior under cyclic lateral loading", *ASCE J. Struct. Eng.*, **133**(3), 378-388. https://doi.org/10.1061/(ASCE)0733-9445(2007)133:3(378)
Purba, R. and Bruneau, M. (2014), Seismic Performance of Steel Plate Shear Walls Considering Various Design Approaches. Technical Report MCEER-14-0005, Multidisciplinary Center for Earthquake Engineering Research, University at Buffalo, State University of New York, Buffalo, NY, USA.
Rahmzadeh, A., Ghassemieh, M., Park, Y. and Abolmaali, A. (2016), "Effect of stiffeners on steel plate shear wall systems", *Steel Compos. Struct., Int. J.*, **20**(3), 545-569. https://doi.org/10.12989/scs.2016.20.3.545
Rahnavard, R., Hassanipour, A. and Mounesi, A. (2016), "Numerical study on important parameters of composite steel-concrete shear walls", *J. Constr. Steel Res.*, **121**, 441-456. https://doi.org/10.1016/j.jcsr.2016.03.017
Rassouli, B., Shafaei, S., Ayazi, A. and Farahbod, F. (2016), "Experimental and numerical study on steel-concrete composite shear wall using light-weight concrete", *J. Constr. Steel Res.*, **126**, 117-128. https://doi.org/10.1016/j.jcsr.2016.07.016
Sabelli, R. and Bruneau, M. (2007), Steel Design Guide 20 – Steel Plate Shear Walls, American Institute of Steel Construction (AISC), USA.
Shafaei, S., Ayazi, A. and Farahbond, F. (2016), "The effect of concrete panel thickness upon composite steel plate shear walls", *J. Constr. Steel Res.*, **117**, 81-90. https://doi.org/10.1016/j.jcsr.2015.10.006
Shafaei, S., Farahbod, F. and Ayazi, A. (2017), "Concrete stiffened steel plate shear walls with an unstiffened opening", *Structures*, **12**, 40-53. https://doi.org/10.1016/j.istruc.2017.07.004
Thorburn, G.L., Kulak, L.J. and Montgomery, C.J. (1983), Analysis of Steel Plate Shear Walls, Structural Engineering Report No. 107; University of Alberta, Edmonton, Alberta, Canada.
Vian, D. (2005), "Steel plate shear walls for seismic design and retrofit of building structures", Ph.D. Dissertation; University of New York at Buffalo, Buffalo, NY, USA.
Wagner, H. (1931), Flat Sheet Metal Girders with Very Thin Webs, Part III: Sheet Metal Girders with Spars Resistant to Bending – The Stress in Uprights – Diagonal Tension Fields, Technical Memorandum No. 606, National Advisory Committee for Aeronautics, Washington, D.C., USA.
Wei, M.W., Liew, J.Y.R., Du, Y. and Fu, X.-Y. (2013), "Seismic behavior of novel partially connected buckling-restrained steel plate shear walls", *Soil Dyn. Earthq. Eng.*, **103**, 64-75. https://doi.org/10.1016/j.soildyn.2017.09.021
Wei, M.-W., Liew, J.Y.R. and Fu, X.-Y. (2017), "Shear resistance of buckling-restrained steel plate shear walls", *Int. J. Steel Struct.*, **17**(3), 1233-1248. https://doi.org/10.1007/s13296-017-9029-2
Willam, K.J. and Warnke, E.D. (1975), "Constitutive Model for the Triaxial Behavior of Concrete", *Proceedings, International Association for Bridge and Structural Engineering*, Vol. 19, ISMES, Bergamo, Italy.
Zhao, Q. (2006), "Experimental and Analytical Studies of Cyclic Behavior of Steel and Composite Shear Wall Systems", Ph.D.

Dissertation, University of California, Berkeley, CA, USA.
Zhao, Q. and Astaneh-Asl, A. (2004), "Cyclic behavior of traditional and innovative composite shear walls", *J. Struct. Eng.*, **130**(2), 271-284. https://doi.org/10.1061/(ASCE)0733-9445(2004)130:2(271)
Zhao, Q. and Astaneh-Asl, A. (2007), "Seismic behavior of composite shear wall systems and application of smart structures technology", *Int. J. Steel Struct.*, **7**(1), 69-75.

CC